Eur Radiol (2011) 21:345–352
DOI 10.1007/s00330-010-1922-4

GASTROINTESTINAL

Does the amount of tagged stool and fluid significantly affect the radiation exposure in low-dose CT colonography performed with an automatic exposure control?

Hyun Kyong Lim · Kyoung Ho Lee · So Yeon Kim · Kil Joong Kim · Bohyoung Kim · Hyunna Lee · Seong Ho Park · Jeffrey H. Yanof · Seung-sik Hwang · Young Hoon Kim

Received: 19 March 2010 / Revised: 29 June 2010 / Accepted: 2 July 2010 / Published online: 11 August 2010

Abstract
Objective To determine whether the amount of tagged stool and fluid significantly affects the radiation exposure in low-dose screening CT colonography performed with an automatic tube-current modulation technique.
Methods The study included 311 patients. The tagging agent was barium (n=271) or iodine (n=40). Correlation was measured between mean volume CT dose index ($CTDI_{vol}$) and the estimated x-ray attenuation of the tagged stool and fluid (*ATT*). Multiple linear regression analyses were performed to determine the effect of *ATT* on $CTDI_{vol}$ and the effect of *ATT* on image noise while adjusting for other variables including abdominal circumference.
Results $CTDI_{vol}$ varied from 0.88 to 2.54 mGy. There was no significant correlation between $CTDI_{vol}$ and *ATT* (p=0.61). *ATT* did not significantly affect $CTDI_{vol}$ (p=0.93), while abdominal circumference was the only factor significantly affecting $CTDI_{vol}$ (p<0.001). Image noise ranged from 59.5 to 64.1 HU. The p value for the regression model explaining the noise was 0.38.
Conclusion The amount of stool and fluid tagging does not significantly affect radiation exposure.

Keywords CT colonography · Radiation dose · Tagging · Automatic exposure control

Introduction

Although CT colonography is now widely accepted as an effective tool for screening for colorectal cancer [1, 2], radiation exposure remains as a drawback. Although debatable, the risk of inducing fatal cancer by means of CT colonography with radiation doses ranging from 4 to 12 mSv has been estimated to be 0.01–0.02% in a 50-year-old individual [3, 4]. The population-based risk in the

H. K. Lim · K. H. Lee (✉) · S. Y. Kim · Y. H. Kim
Department of Radiology,
Seoul National University Bundang Hospital,
300 Gumi-dong, Bundang-gu,
Seongnam-si, Gyeonggi-do, 463-707, Korea
e-mail: kholeemail@gmail.com

H. K. Lim · K. H. Lee · S. Y. Kim · Y. H. Kim
Institute of Radiation Medicine,
Seoul National University College of Medicine,
Seoul National University Medical Research Center,
Bundang, Korea

K. J. Kim
Department of Radiation Applied Life Science,
Seoul National University College of Medicine,
Seoul, Korea

B. Kim · H. Lee
School of Computer Science and Engineering,
Seoul National University,
Seoul, Korea

S. H. Park
Department of Radiology and Research Institute of Radiology,
Asan Medical Center, University of Ulsan College of Medicine,
Seoul, Korea

J. H. Yanof
Philips Healthcare, CT Clinical Science,
Cleveland, OH, USA

S.-s. Hwang
Department of Social & Preventive Medicine,
Inha University School of Medicine,
Incheon, Korea

future might not be negligible, considering the increased use of screening CT colonography.

The use of automatic exposure control (AEC) techniques [5] enables a significant reduction in radiation exposure without loss of image quality in CT colonography [6] as in any other CT applications. The principle of the AEC techniques is to adjust *x*-ray intensity according to regional *x*-ray attenuation in the body, thereby adapting radiation exposure for individual patients while maintaining constant image quality. However, when the region undergoing imaging contains a highly attenuating material, the AEC techniques can overcompensate suggesting excessive radiation exposure. For instance, it has been reported that the presence of a metallic prosthesis is associated with a 34.1% increase in the radiation exposure in abdominal–pelvic CT obtained with an AEC technique [7].

For CT colonography, a similar concern regarding the excessive radiation exposure can be raised if an AEC technique is used in conjunction with stool or fluid tagging agents such as barium or iodine. The use of the tagging agents is essential to reduce false-positive diagnoses, especially if the colon is to be cleansed in a less vigorous manner to improve patient compliance in a screening programme [8]. The presence of large amounts of the highly attenuating material in the bowel might result in an inadvertent increase in the radiation exposure by an AEC technique.

Our study aimed to determine whether the amount of tagged stool and fluid significantly affects the radiation exposure in low-dose screening CT colonography performed with an AEC technique.

Materials and methods

Our institutional review board approved this prospective study and waived the patient informed consent as all CT were obtained following our clinical protocol and patient confidentiality was maintained. One author is an employee of Philips Healthcare, the manufacturer of the imaging device used in this study. Those authors who are not employees of Philips Healthcare had control of the data and the information submitted for publication and control of inclusion of any data and information that might present a conflict of interest for the author who is an employee for Philips Healthcare.

Study sample

The study initially included 316 consecutive patients screened with low-dose CT colonography in our institution between August 2008 and November 2008. The rationale for the sample size determination is described in Appendix 1. The patients were typically asymptomatic and had average risk of colorectal cancer. By reviewing the CT colonography images, a study coordinator excluded three patients with metallic prosthesis within the imaging range. Additionally, two patients were excluded as the imaging showed severe motion artefacts hindering subsequent measurement of the tagged stool and fluid by using image post-processing techniques (described below).

The remaining 311 patients (age range, 40–82 years; mean±SD, 54.7±8.2 years) were finally included (Fig. 1). They were 179 men (40–82; 54.0±8.0 years) and 132 women (40–81; 55.6±8.4 years). The abdominal circumference (cm) at the umbilicus level was measured for each patient.

Bowel preparation

For CT colonography, the selection of the cathartic agent and tagging agent was made at the discretion of the referring physician, considering the patients' physical state, particularly the renal and cardiovascular functions. In 271 patients who were administered magnesium citrate (50 g Magcorol powder; Taejoon Pharmaceutical, Seoul, Korea) (n=252) or sodium phosphate (n=19) (90 mL Colclean; Taejoon Pharmaceutical) for bowel cleansing, three doses of 200 mL of 4.6% w/v barium (EZ-CT; Taejoon Pharmaceutical) were used for stool tagging. In the remaining 40 patients who were administered polyethylene glycol electrolyte (4 L Colyte-F; Taejoon Pharmaceuticals), a single dose of 100 mL of water-soluble iodine agent (diatrizoate meglumine and diatrizoate sodium; Gastrografin, Bracco Diagnostics, Princeton, NJ, USA) was used for fluid tagging. All patients were prescribed low-residue diet on the day before CT colonography and were administered 10 mg of bisacodyl suppository (Dulcolax; Boehringer Ingelheim, Seoul, Korea) in the morning on the day of the examination.

CT colonography

An automated CO_2 delivery system (PROTOCO2L; E-Z-Em, Westbury, NY, USA) was used. No spasmolytics were used. Non-contrast low-dose prone and supine

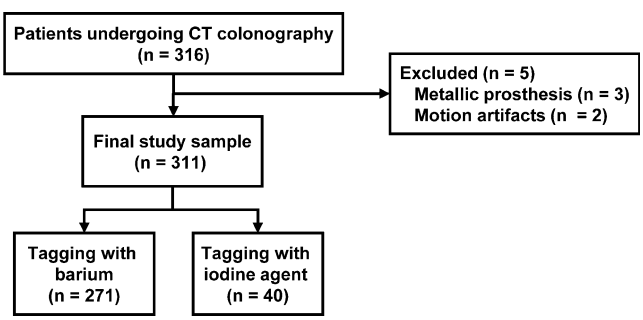

Fig. 1 Patient flow diagram

acquisitions were obtained using 64-detector-row CT equipments (Brilliance; Philips Healthcare, Cleveland, OH, USA) with the use of an AEC system. Transverse CT images were reconstructed with the section thickness of 0.67 mm and the reconstruction interval of 0.6 mm. Other imaging parameters are tabulated in Table 1. Mean volume CT dose index, $CTDI_{vol}$ (mGy), was recorded for each of the prone and supine helical scans. The AEC maintains approximately the same preferred image noise level across patients (patient-to-patient modulation; Automatic Current Selection [ACS], Philips Healthcare) and across images along the craniocaudal axis within an acquisition (*z*-axis modulation [Z-DOM]; Philips Healthcare) (Appendix 2). We did not use an angular modulation, as simultaneous *z*-axis and angular modulations were not available for the imaging device we used and the vendor recommended choosing the former rather than the latter. The effective dose of the prone and supine scans, estimated by multiplying the dose-length products reported on the CT console by a conversion factor (0.017 $mSv{\cdot}mGy^{1}{\cdot}cm^{1}$) [9], was 1.3–4.7 (mean±SD, 2.3±0.6) mSv. This radiation dose level was empirically determined for our Asian population based on our previous experience [10]. The images were interpreted as part of routine practice, as described elsewhere [10]. We did not analyse the diagnostic performance, as it was not the purpose of our study.

Tagged stool and fluid

From the image dataset of each prone or supine image, the study coordinator segmented the voxels corresponding to the tagged stool and fluid remaining inside the colon as well as the other segments of the alimentary tract with a semi-automatic method (Fig. 2, Appendix 3). Although either the barium or iodine agent was used in each patient, it was considered that each tagging agent could tag both residual stool and fluid. From the segmentation results, a computer scientist calculated the volume (*vol*) (cm^3) as well as the mean (HU_{mean}) and median (HU_{median}) CT numbers (HU) of the tagged stool and fluid using the Matlab program (version R2007a, MathWorks, Natick, MA, USA). In addition, the *x*-ray attenuation by the tagged stool and fluid (*ATT*) was estimated with the Beer-Lambert law as $e^{\mu_{water}\times\left(1+\frac{HU_{mean}}{1000}\right)\times\sqrt{[3]vol}}$, where μ_{water} is the linear attenuation coefficient of water (0.193 cm^{-1}) [11] (Appendix 4).

Image noise

Although the AEC mechanisms we used were designed to maintain an approximately constant image noise level [5, 12], this constancy was assessed with two separate analyses.

First, the image noise was quantitatively measured as the standard deviation of CT numbers of intracolonic air voxels segmented from the images using a semi-automatic method by the study coordinator (Fig. 2, Appendix 3). We chose to measure the image noise in the intracolonic air rather than in the background air outside the body, as the former is more relevant than the latter in assessing the quality of three-dimensional (3D) endoluminal fly-through images.

Second, two independent radiologists visually assessed the irregularity of the endoluminal surface of the colon, as an indicator of the image noise. Each radiologist had experience of interpretation of at least 700 CT colonography examinations. The radiologists were unaware of the study design and blinded to the measured image noise. This subjective analysis was performed in a retrospective manner to maintain consistency in the radiologists' visual assessment. As this analysis aimed to confirm that the image noise level was approximately constant across the patients, we included only 20 patients, ten patients with the lowest image noise measurements (the mean of prone and supine scans) and ten patients with the highest image noise measurements. The order of patients was randomised for each radiologist. After a complete 3D fly-through review (rectum-to-cecum and cecum-to-rectum for the prone and supine images), each radiologist graded the surface irregularity on a four-grade scale: grade 0, very smooth and shiny surface; grade 1, slightly irregular surface, but polyp detection would not be affected; grade 2, the detection of a flat polyp can be potentially affected because of the irregular surface; and grade 3, unacceptable quality due to the severely irregular surface. Visualisation parameters of the reviewing software (Aquarius, Terarecon, San Mateo, CA, USA) were set to default settings.

Table 1 Imaging parameters

Parameter	Comments
Tube parameters	Tube potential, 120 kVp; effective tube current-time product, 13–57 mAs
Dose modulation program	Automatic Current Selection and *z*-axis modulation
Gantry rotation	Rotation time, 0.42 sec; pitch, 1.25
Collimation	64×0.625 mm
Reconstruction	Reconstruction thickness, 0.67 mm; reconstruction interval, 0.6 mm; standard soft tissue filter

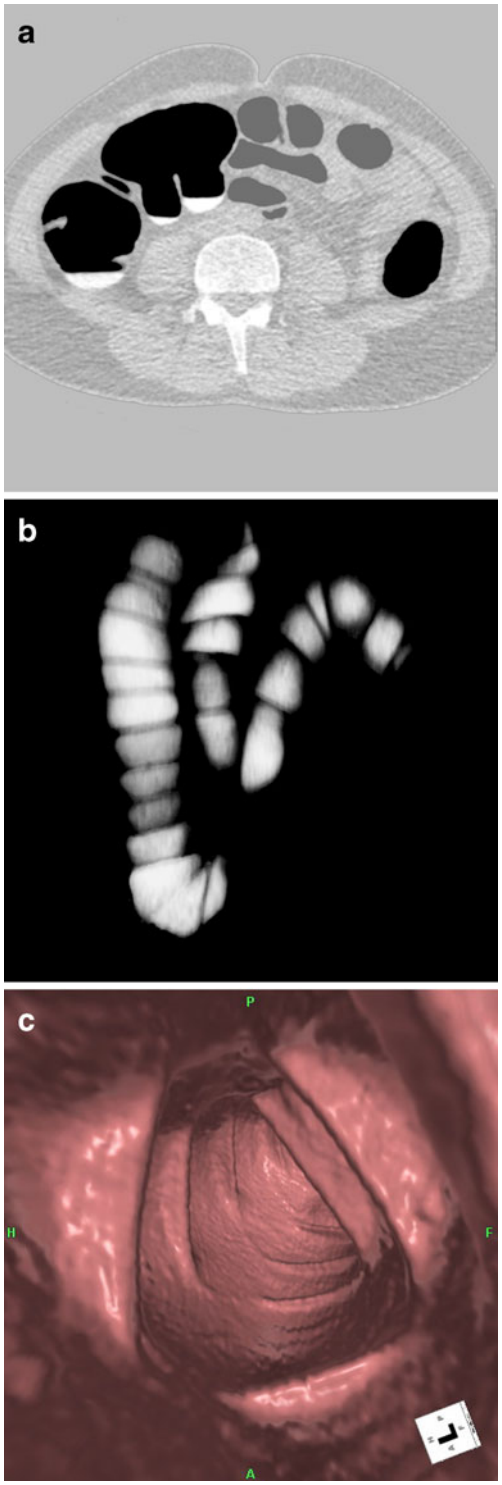

◀ **Fig. 2** Segmentation results in a 57-year-old woman. **a** Transverse CT colonography image. Dark and grey areas indicate segmented air inside the colon and small bowel, respectively. **b** Volume rendering image of segmentation results for tagged stool and fluid inside the alimentary tract. The measured *vol*, HU_{mean}, HU_{median} and *ATT* were 64.2 cm^3, 411.2 HU, 416.0 HU, and 2.97, respectively. **c** Endoluminal image. The surface irregularity was rated as grade 1 by both radiologists. *ATT*, estimated *x*-ray attenuation by the tagged stool and fluid; HU_{mean}, mean CT number of the tagged stool and fluid; HU_{median}, median CT number of the tagged stool and fluid; *vol*, volume of the tagged stool and fluid.

Statistical analysis

For all measurements (*vol*, HU_{mean}, HU_{median}, image noise and $CTDI_{vol}$), the mean values of the prone and supine scans were used in the statistical analyses. The Pearson correlation was measured between $CTDI_{vol}$ and each of *vol*, HU_{mean}, HU_{median} and *ATT* of the tagged stool and fluid.

For the variables with skewed data distribution, natural logarithm or square root transforms of the data were used instead of the original data. $CTDI_{vol}$, *vol* and *ATT* were transformed to $ln(CTDI_{vol})$, $\sqrt{vol}$ and *ln(ATT)*, respectively.

Multiple linear regression analysis was used to determine the effect of *ATT* on $CTDI_{vol}$ while adjusting for other variables including age, sex, abdominal circumference and the type of tagging agent. In a similar manner, another multiple linear regression analysis was performed to determine the effect of *ATT* on the image noise, while adjusting for other variables including age, sex, abdominal circumference, the type of tagging agent and $CTDI_{vol}$. The *vol*, HU_{mean} and HU_{median} did not enter the multiple linear regression models because they were represented by *ATT*. To ensure linearity between the continuous variables included in the multiple linear regressions, the noise and abdominal circumference were transformed to $\frac{1}{noise^2}$ and $e^{0.719\times\mu_{water}\times\left(\frac{abdominal\ circumference}{\pi}-32\right)}$, respectively, before entering the regression models (Appendix 4). A p value of <0.05 was considered to indicate statistical significance. Statistical software (SPSS, version 15.0; SPSS, Chicago, IL, USA) was used.

Finally, the concordance rate was measured for the two radiologists' grading results.

Results

Correlation

$CTDI_{vol}$ varied from 0.88 to 2.54 (mean±SD, 1.45±0.32) mGy. The mean *vol*, HU_{mean}, HU_{median} and *ATT* were 61.2 cm^3, 403.9 HU, 388.6 HU and 2.72, respectively (Table 2). There was no significant correlation between $ln(CTDI_{vol})$ and each of $\sqrt{vol}$ (r=−0.03 [95% CI, −0.14, 0.08], p=0.59), HU_{mean} (r=−0.08 [−0.20, 0.03], p=0.15), HU_{median} (r=−0.09 [−0.20, 0.02], p=0.11), and *ln(ATT)* (r=−0.03 [−0.14, 0.08], p=0.61).

The effect of *ATT* on $CTDI_{vol}$

The results of the multiple linear regression analysis showed that *ATT* did not significantly affect $CTDI_{vol}$ (p=0.93) when

Table 2 Measured data

Variable	Mean±SD	25th, 50th, and 75th percentiles	Range
vol (cm^3)	61.2±82.5	9.0, 34.0, 79.7	0–574.9
HU_{mean} (HU)[a]	403.9±94.4	346.6, 396.0, 464.2	211.1–752.3
HU_{median} (HU)[a]	388.6±92.0	321.8, 386.1, 441.8	210.2–688.8
ATT	2.72±1.49	1.74, 2.41, 3.33	1–12.80
Abdominal circumference	84.6±8.1	80.3, 85.1, 90.2	59.0–102.0
$CTDI_{vol}$ (HU)	1.45±0.32	1.22, 1.40, 1.63	0.88–2.54
Image noise (mGy)	61.5±0.9	60.8, 61.4, 62.1	59.5–64.1

[a] Could not be measured in 12 patients with *vol* of 0. *ATT*, estimated *x*-ray attenuation by the tagged stool and fluid; $CTDI_{vol}$, mean volume CT dose index; HU_{mean}, mean CT number of the tagged stool and fluid; HU_{median}, median CT number of the tagged stool and fluid; *vol*, volume of the tagged stool and fluid

the other four variables were adjusted. Of the tested variables, the transform of abdominal circumference (Table 2), $e^{0.719\times\mu_{water}\times\left(\frac{abdominal\ circumference}{\pi}-32\right)}$, was the only factor significantly affecting $CTDI_{vol}$ ($p<0.001$) (Table 3).

The effect of *ATT* on Image Noise

The image noise measured in the intracolonic air regions ranged from 59.5 to 64.1 (mean±SD, 61.5±0.9) HU (Table 2). The regression model including *ATT* and the five other variables did not explain the transform of noise, $\frac{1}{noise^2}$, in a statistically significant manner ($R^2=0.02$, $p=0.38$).

Visual analysis

The visual analysis included the ten patients with the lowest image noise measurements (range, 59.5–59.7 HU) and the ten patients with the highest image noise measurements (63.2–64.1 HU). One of the two radiologists rated the surface irregularity in all 20 cases as grade 1 (Fig. 2). The other radiologist rated the surface irregularity as grade 1 in 19 cases and as grade 2 in one patient who had a measured noise level of 63.2 HU. The concordance rate between the two radiologists was 95% (19/20).

Table 3 Results of multiple linear regression analysis for variables affecting $CTDI_{vol}$

Variable	Coefficient (β)	*p* value
Intercept	1.00 (0.75, 1.26)	<0.001
Age (y)	−0.00 (−0.01, 0.00)	0.19
Sex (male)	0.02 (−0.04, 0.08)	0.46
Abdominal circumference (cm)[a]	1.17 (1.01, 1.33)	<0.001
Tagging agent (barium)	−0.04 (−0.12, 0.04)	0.34
ATT[a]	−0.00 (−0.02, 0.02)	0.93

Data in parenthesis are 95% CIs. $R^2=0.43$ ($p<0.001$). [a] Transformed or estimated according to Appendix 4. *ATT*, estimated *x*-ray attenuation by the tagged stool and fluid; $CTDI_{vol}$, mean volume CT dose index

Discussion

In our results, $CTDI_{vol}$ varied from 0.88 to 2.54 (mean±SD, 1.45±0.32) mGy, while the image noise was maintained within the range of 59.5 to 64.1 (mean±SD, 61.5±0.9) HU, and the radiologists rated the surface irregularity as grade 1 in all but one of the 20 tested cases. These results indicate that the AEC technique adapted radiation exposure for individual patients appropriately to maintain approximate constancy of the image noise.

There was no significant correlation between $ln(CTDI_{vol})$ and each of the parameters $\sqrt{vol}$, HU_{mean}, HU_{median} and $ln(ATT)$. The regression analysis showed that *ATT* did not significantly affect $CTDI_{vol}$. These results indicate that the amount of tagged stool and fluid did not significantly affect the radiation exposure. Therefore, when the stool or fluid tagging technique was used, the concern regarding excessive radiation exposure due to overcompensation of the AEC was not substantiated.

Our results demonstrating an insignificant effect of the amount of the tagged stool and fluid on the radiation exposure might be considered counterintuitive, as tagged stool and fluid should contribute to the overall *x*-ray attenuation of the region undergoing imaging. A plausible explanation for our results would be that the attenuation by the tagged stool and fluid might be considerably small, or even negligible, compared with the attenuation by the patient's body. In other words, the AEC system might not be precise enough to respond to a small change in the *x*-ray attenuation by the tagged stool and fluid, though the system competently responded to the relatively larger change in the *x*-ray attenuation according to the patient's body size. In theory, an excessive amount of tagged stool and fluid could potentially increase the radiation exposure, as does a metallic prosthesis [7]. Therefore, it is unclear whether our results can be reproduced in patients with different colon preparations leaving more residues of tagging agents by using no cathartic agent or by tagging with both barium and iodine agents. Nevertheless, it should be noted that our results can be still generalised to patients undergoing bowel preparations similar to the regimens used in our study.

Our study has limitations. First, we used imaging devices of a single type. We did not use angular modulation as simultaneous *z*-axis and angular modulations were not available for the imaging device we used. Investigations testing other types of device capable of such simultaneous modulations are needed to further generalise our results. Second, the analysis of image quality with regard to the image noise relied on the radiologists' subjective rating for the surface irregularity. It would have been ideal if polyp detection performance could have been evaluated to corroborate the finding that the image noise level was maintained within an acceptable range. However, we were unable to perform such an analysis because many patients did not undergo subsequent optical colonoscopy.

Our study demonstrated that the amount of tagged stool and fluid did not significantly affect the radiation exposure in low-dose screening CT colonography performed with an AEC technique. In patients undergoing bowel preparations similar to the regimens used in our study, the concern regarding excessive radiation exposure by overcompensation of the AEC can be mitigated when a stool or fluid tagging technique is used.

Acknowledgment This work was supported by the Korea Science and Engineering Foundation (KOSEF) grant funded by Ministry of Science and Technology (MOST), Republic of Korea (No. R01-2008-000-10055-0).

Appendix 1. Sample Size Determination

A recent study [13] evaluating an AEC mechanism reported a correlation coefficient (r) of 0.83 for the correlation between the mean effective tube current level and body mass index in abdomen and pelvis CT studies for general purposes. Based on these data, we assumed 0.7 as R^2 of the regression model in our study if $CTDI_{vol}$ is predicted from the four tested variables other than the *ATT*. To achieve 90% power to detect an R^2 increase of 0.01 attributed to the *ATT*, the sample size was estimated as 310 using an F-test with a significance level (alpha) of 0.05. Allowing for a dropout rate of 2%, the sample size was finally determined as 316.

Appendix 2. Mechanism of the AEC Techniques

The mechanism of the AEC techniques we used (ACS and Z-DOM) is as follows. The topogram is used to estimate *x*-ray attenuation (measured as water-equivalent diameter, D_w) by the patient body at each table position in the imaging range. From the set of D_w, the system assesses the overall size of the patient cross-section, compares the body size with a predetermined standard body size, and adjusts the tube current for the patient. If the estimated body size is larger or smaller than the standard body size, the suggested tube current would be increased or decreased, respectively. In general, the tube current is doubled for every 5-cm increase in the transverse diameter of body. In addition, the tube current is modulated along the *z*-axis (longitudinal) of the patient, based on the profile of D_w along the *z*-axis. The technical details and validation results are available elsewhere [5, 12].

Appendix 3. Segmentation Methods

The study coordinator segmented intracolonic air as well as tagged stool and fluid remaining inside the alimentary tract using a semi-automatic method. Custom software was used, which was modified from commercial 3D visualisation software (Xelis; Infinitt Healthcare, Seoul, Korea) by two of the authors. The software employed commonly used image post-processing techniques such as connected component labelling and 3D region growing [14, 15]. The software operated on a PC platform running Windows XP (Microsoft Co., Redmond, WA, USA) with a 2-GHz dual-core processor (Xeon 5130; Intel Co., Santa Clara, CA, USA) and a 3-Gbyte main memory.

Voxels corresponding to intracolonic air were segmented using 3D seeded region-growing techniques [16, 17] as follows. First, the patient's body region was extracted. Second, the voxels of the lungs were removed to avoid leakage into the lungs during the segmentation of the intraluminal air regions in the subsequent step. Third, the voxels of the air inside the alimentary tract were segmented by selecting voxels with CT numbers smaller than −800 HU [18]. Fourth, only large connected components were selected to identify intracolonic air. Finally, the radiologist approved or discarded each of the segmented air columns by reviewing the automatic segmentation results.

The algorithm used to segment tagged fluid or stool was as follows. First, the axial skeleton was removed to avoid leakage into the bone in the subsequent 3D region-growing step [14]. Second, as the previously segmented volume of air inside the alimentary tract (the colon as well as the other segments of the alimentary tract) was gradually enlarged using a morphology operator, dilation [19], to 20 mm from its original boundary, voxels greater than 200 HU [20] were identified. Third, these voxels served as seed points for 3D region growing [14] to find neighbouring voxels greater than 200 HU. Finally, the radiologist reviewed and approved the segmentation results by manually adding new seed points and discarding incorrectly segmented regions.

Appendix 4. Variable Transformation

To ensure the linearity between the continuous variables included in the multiple linear regressions, each of the variables was transformed to be linear to the intensity of the incident *x*-ray (I_0) before entering the regression models.

$CTDI_{vol}$

By definition, $CTDI_{vol}$, as measured with a standard 32-cm body phantom, is linear to I_0.

Image noise

Image noise, defined as the standard deviation of CT numbers in the region of intracolonic air, is inversely proportional to the square root of the number of *x*-ray quanta [21] to which I_0 is linearly related. Therefore, noise and I_0 have the following relationship:

$$I_0 \propto \frac{1}{noise^2}.$$

Abdominal circumference

According to the Beer-Lambert law, the *x*-ray attenuation by the patient body can be approximately described as follows,

$$I = I_0 \times e^{-\mu_{water} \times l}, \tag{A1}$$

where I is the intensity of the transmitted x-ray, μ_{water} is the linear attenuation coefficient of water, and l is the diameter of the patient's abdomen.

The AEC generally doubles I_0 for every 5-cm increase in the estimated diameter of the abdomen. Therefore, assuming that the transverse section of the abdomen has a circular shape, the Eq. A1 can be transformed as follows:

$$I = I_0 \times e^{-f \times \mu_{water} \times \left(\frac{abdominal\ circumference}{\pi} - D_{ref}\right)}, \tag{A2}$$

where f is a constant, 0.719, selected for the tube current doubling rate and D_{ref} is a reference diameter stored as 32 cm in the imaging protocol. As I can be regarded as an approximately constant value when the AEC operates competently, abdominal circumference and I_0 have the following relation:

$$I_0 \propto e^{f \times \mu_{water} \times \left(\frac{abdominal\ circumference}{\pi} - D_{ref}\right)}$$

ATT

The *x*-ray attenuation by the tagged stool and fluid can be described as follows:

$$I_t = I_0 \times e^{-\mu_t \times l_t}, \tag{A3}$$

where I_t is the intensity of the *x*-ray transmitted through the tagged stool and fluid, μ_t is the mean linear attenuation coefficient of tagged stool and fluid, and l_t is the length of the tagged stool and fluid along the *x*-ray path. Assuming that the tagged stool and fluid are randomly distributed in the volume undergoing imaging, the Eq. A3 can be transformed as follows:

$$I_0 = I_t \times e^{\mu_t \times \sqrt{[3]vol}}, \tag{A4}$$

where *vol* is the volume of the tagged stool and fluid.

As $\mu_t = \mu_{water} \times \left(1 + \frac{HU_{mean}}{1000}\right)$, where HU_{mean} is the mean CT number of the voxels of the tagged stool and fluid, the Eq. A4 can be transformed as follows:

$$I_0 = I_t \times e^{\mu_{water} \times \left(1 + \frac{HU_{mean}}{1000}\right) \times \sqrt{[3]vol}}. \tag{A5}$$

As I_t is held approximately constant by the AEC, $e^{\mu_{water} \times \left(1 + \frac{HU_{mean}}{1000}\right) \times \sqrt{[3]vol}}$ is linear to I_0. Therefore, $e^{\mu_{water} \times \left(1 + \frac{HU_{mean}}{1000}\right) \times \sqrt{[3]vol}}$ was used as an independent describing *ATT*.

References

1. Johnson CD, Chen MH, Toledano AY, Heiken JP, Dachman A, Kuo MD, Menias CO, Siewert B, Cheema JI, Obregon RG, Fidler JL, Zimmerman P, Horton KM, Coakley K, Iyer RB, Hara AK, Halvorsen RA Jr, Casola G, Yee J, Herman BA, Burgart LJ, Limburg PJ (2008) Accuracy of CT colonography for detection of large adenomas and cancers. N Engl J Med 359:1207–1217
2. Levin B, Lieberman DA, McFarland B, Smith RA, Brooks D, Andrews KS, Dash C, Giardiello FM, Glick S, Levin TR, Pickhardt P, Rex DK, Thorson A, Winawer SJ (2008) Screening and surveillance for the early detection of colorectal cancer and adenomatous polyps, 2008: a joint guideline from the American Cancer Society, the US Multi-Society Task Force on Colorectal Cancer, and the American College of Radiology. CA Cancer J Clin 58:130–160
3. Brenner DJ, Georgsson MA (2005) Mass screening with CT colonography: should the radiation exposure be of concern? Gastroenterology 129:328–337
4. van Gelder RE, Venema HW, Serlie IW, Nio CY, Determann RM, Tipker CA, Vos FM, Glas AS, Bartelsman JF, Bossuyt PM, Lameris JS, Stoker J (2002) CT colonography at different radiation dose levels: feasibility of dose reduction. Radiology 224:25–33
5. Keat N (2005) Report 05016: CT scanner automatic exposure control systems. Available via http://www.impactscan.org/reports/Report05016. Accessed Mar 28 2010
6. Graser A, Wintersperger BJ, Suess C, Reiser MF, Becker CR (2006) Dose reduction and image quality in MDCT colonography using tube current modulation. Am J Roentgenol 187:695–701
7. Rizzo SM, Kalra MK, Maher MM, Blake MA, Toth TL, Saini S (2005) Do metallic endoprostheses increase radiation dose associated with automatic tube-current modulation in abdominal-pelvic MDCT? A phantom and patient study. Am J Roentgenol 184:491–496

8. Hara AK (2002) The future of colorectal imaging: computed tomographic colonography. Gastroenterol Clin North Am 31:1045–1060
9. Bongartz G, Golding SJ, Jurik AG, Leonardi M, van Meerten EvP, Geleijns J, Jessen KA, Panzer W, Shrimpton PC, Tosi G (2004) European guidelines on quality criteria for computed tomography. Report EUR 16262. Available via http://www.drs.dk/guidelines/ct/quality/index.htm. Accessed Mar 28 2010
10. An S, Lee KH, Kim YH, Park SH, Kim HY, Kim SH, Kim N (2008) Screening CT colonography in an asymptomatic average-risk Asian population: a 2-year experience in a single institution. Am J Roentgenol 191:W100–W106
11. Hsieh J (2003) Preliminaries. In: Hsieh J (ed) Computed tomography: principles, design, artifacts, and recent advances. SPIE Optical Engineering Press, Bellingham, WA, p 34
12. Soni NK, Cohn NA (2009) Strategies to reduce radiation dose in Philips multidetector computed tomography scanners. In: Mahesh M (ed) MDCT physics: the basics-technology, image quality and radiation dose. Lippincott Williams & Wilkins, Philadelphia, PA, pp 125–130
13. Mulkens TH, Bellinck P, Baeyaert M, Ghysen D, Van Dijck X, Mussen E, Venstermans C, Termote JL (2005) Use of an automatic exposure control mechanism for dose optimization in multi-detector row CT examinations: clinical evaluation. Radiology 237:213–223
14. Adams R, Bischof L (1994) Seeded region growing. IEEE Trans Pattern Anal Mach Intell 16:641–647
15. Gonzalez RC, Woods RE (1992) Region-oriented segmentation. In: Gonzalez RC, Woods RE (eds) Digital image processing. Addison-Wesley Publishing Company, Reading, MA, pp 458–465
16. Lee J, Kim G, Lee H, Shin B-S, Shin YG (2008) Fast path planning in virtual colonoscopy. Comput Biol Med 38:1012–1023
17. Wyatt CL, Ge Y, Vining DJ (2000) Automatic segmentation of the colon for virtual colonoscopy. Comput Med Imaging Graph 24:1–9
18. Summers RM, Franaszek M, Miller MT, Pickhardt PJ, Choi JR, Schindler WR (2005) Computer-aided detection of polyps on oral contrast-enhanced CT colonography. Am J Roentgenol 184:105–108
19. Gonzalez RC, Woods RE (1992) Dilation and erosion. In: Gonzalez RC, Woods RE (eds) Digital image processing. Addison-Wesley Publishing Company, Reading, MA, pp 518–524
20. Zalis ME, Perumpillichira JJ, Magee C, Kohlberg G, Hahn PF (2006) Tagging-based, electronically cleansed CT colonography: evaluation of patient comfort and image readability. Radiology 239:149–159
21. Prokop M (2003) Image analysis. In: Prokop M, Galanski M (ed) Computed tomography of the body. Georg Thieme Verlag, Stuttgart, Germany, p 143